Nuclear spin state narrowing via gate—controlled Rabi oscillations in a double quantum dot

D. Klauser, W. A. Coish, and Daniel Loss

Department of Physics and Astronomy, University of Basel,

Klingelbergstrasse 82, CH-4056 Basel, Switzerland

(Dated: December 2, 2024)

We study spin dynamics for two electrons confined to a double quantum dot under the influence of an oscillating exchange interaction. This leads to driven Rabi oscillations between the $|\uparrow\downarrow\rangle$ -state and the $|\downarrow\uparrow\rangle$ -state of the two-electron system. The width of the Rabi resonance is proportional to the amplitude of the oscillating exchange. A measurement of the Rabi resonance allows one to narrow the distribution of nuclear spin states and thereby to prolong the spin decoherence time. Further, we study decoherence of the two-electron states due to the hyperfine interaction and give requirements on the parameters of the system in order to initialize in the $|\uparrow\downarrow\rangle$ -state and to perform a $\sqrt{\text{SWAP}}$ operation with unit fidelity.

PACS numbers: 73.21.La,76.20.+q,76.30.-v,85.35.Be

I. INTRODUCTION

One of the important proposals for quantum information processing in solid–state systems is the spin–qubit proposal for quantum computing with electron spins in quantum dots¹. Much effort has been put into the realization of this proposal leading to exciting theoretical² and experimental achievements.^{3,4,5,6,7,8,9} Still many challenges remain such as decoherence and the implementation of single–qubit gates.

A major obstacle to quantum computation with the quantum dot spin-qubit is decoherence due to the coupling of the qubit to its environment. The hyperfine interaction between the electron spin and the nuclear spins present in all III-V semiconductors¹⁰ leads to the strongest decoherence effect^{9,11,12,13,14,15,16,17,18} Experiments^{8,9,19,20} have yielded values for the freeinduction spin dephasing time T_2^* that are consistent with $T_2^* \sim \sqrt{N}/A \sim 10 {\rm ns}^{14,15,16}$ for $N=10^6$ and $A = 90 \mu \text{eV}$ in GaAs, where N is the number of nuclei within one quantum dot Bohr radius and A characterizes the hyperfine coupling strength.²¹ This is to be contrasted to potential spin-echo envelope decay, which may be much larger. ^{22,23,24} With a two-qubit switching time of $\tau_s \sim 50 \mathrm{ps}^{11}$ this only allows $\sim 10^2$ gate operations within T_2^* , which falls short (by a factor of 10 to 10²) of current requirements for efficient quantum error ${\it correction.}^{25}$

There are several ways to overcome the problem of hyperfine-induced decoherence of which measurement and thus projection of the nuclear spin state seems to be the most promising one¹⁷. Other methods include polarization^{11,16,17,26} of the nuclear spins and spin echo techniques.^{9,17,23} However, in order to extend the decay time by an order of magnitude through polarization of the nuclear spins a polarization of above 99% is required,¹⁷ but the best result so far reached is only $\sim 60\%$ in quantum dots.^{3,19} With spin-echo techniques, gate operations still must be performed within the single-

spin free—induction time, which requires faster gate operations. A projective measurement of the nuclear spin state leads to an extension of the decay time for the spin. This extension is only limited by the ability to do a strong measurement since the longitudinal nuclear spin in a quantum dot is expected to survive up to the spin diffusion time, which is on the order of seconds for nuclear spins surrounding donors in GaAs.²⁷

The implementation of quantum computation schemes requires coherent control of the qubits. Rabi oscillations between the two qubit states are an important signature of coherence and thus observation of controlled Rabi oscillations is an important intermediate step in the experimental implementation of quantum information processors. Despite recent experimental achievements^{3,9} there still lacks the experimental observation of driven Rabi oscillations for a system of two quantum dot spin–qubits. What has been observed is electron spin resonance via g-tensor modulation in a bulk semiconductor.²⁸

In the quantum dot spin–qubit proposal two–qubit gates are realized through tuning of the exchange coupling between the two spins. 1,11 In devices such as those in Refs. 8,9 this exchange coupling is given by the splitting J between singlet and triplet states of the two–electron system and can be controlled through gate voltages. Petta $et\ al.^9$ have very recently managed to implement the $\sqrt{\rm SWAP}$ –gate in their setup. In order to implement single–qubit gates, control over local magnetic fields or g–factors is required. 11

As we will show in Sec.II, an oscillating exchange J(t) induces Rabi oscillations between the states $|\uparrow\downarrow\rangle$ and $|\downarrow\uparrow\rangle$ of two electron spins (one electron on each dot). The amplitude of these oscillations is resonant on the splitting between $|\uparrow\downarrow\rangle$ and $|\downarrow\uparrow\rangle$ and the width of this resonance is proportional to the amplitude j of the oscillating component of J(t). Since the splitting depends on the state of the nuclear system, a measurement of the resonance is also a measurement of the state of the nuclear spins and thus provides a way to narrow the quantum distribution of the nuclear spin states. This narrowing of the

spin state is one possible solution to suppress hyperfine—induced decoherence in quantum dot spin-qubits¹⁷. It has been proposed to measure the nuclear spin polarization using a phase estimation method.²⁹ In the ideal case, phase estimation yields one bit of information about the nuclear spin system for each perfectly measured electron. Optical methods have also been proposed.³⁰ The all–electrical method we present here only requires a single sweep of j and can be applied with current technology.

The rest of this paper is organized as follows. In Sec. II we show that an oscillating exchange leads to driven Rabi oscillations and calculate the resonance linewidth. Further, we propose a scheme to narrow the distribution of the nuclear spin states. In Sec. III we consider decoherence induced through the hyperfine interaction for a static exchange coupling J. We use these results in Sec.IV to analyze under which conditions we reach unit fidelity for the initialization to the state $|\uparrow\downarrow\rangle$ and a $\sqrt{\text{SWAP}}$ operation. Sec. V contains a summary of our results.

II. OSCILLATING EXCHANGE AND ESR

In this section we show that under suitable conditions an oscillating exchange interaction may be used to induce Rabi oscillations in a system of two electrons confined to a double quantum dot like those in Refs. 6,7,8,9.

We denote by $\mathbf{h}_i = (h_i^x, h_i^y, h_i^z)$, i = 1, 2, the collective quantum nuclear spin operator, the "Overhauser operator", in dot one and two, respectively, and write $\delta h^z = \frac{1}{2}(h_1^z - h_2^z)$. Further, $\langle \mathcal{O} \rangle_{\rm rms} = \langle \psi_I | \mathcal{O}^2 | \psi_I \rangle^{1/2}$ is the root–mean–square expectation value of the operator \mathcal{O} with respect to the nuclear spin state $|\psi_I\rangle$. We assume that the Zeeman splitting $\epsilon_z = g\mu_B B$ induced by a uniform applied magnetic field $\mathbf{B} = (0, 0, B)$, B > 0 is much larger than $\langle \delta \mathbf{h} \rangle_{\rm rms}$ and $\langle \mathbf{h}_i \rangle_{\rm rms}$. Under these conditions the relevant spin Hamiltonian becomes block diagonal with blocks labeled by to the total electron spin projection along the magnetic field S^z . In the subspace of $S^z = 0$ the Hamiltonian can be written as $(\hbar = 1)^{18}$

$$H_0 = \frac{J}{2} \left(1 + \tau^z \right) + \delta h^z \tau^x + \delta b^z \tau^x. \tag{1}$$

Here, J is the Heisenberg exchange coupling between electron spins on the two dots and δb^z the inhomogeneity of an externally applied classical magnetic field which we add, in addition to the treatment in Ref. 18. Further, $\boldsymbol{\tau}=(\tau^x,\tau^y,\tau^z)$ is the vector of Pauli matrices in the basis of $S^z=0$ singlet $|S\rangle$ and triplet $|T_0\rangle$ ($|S\rangle \rightarrow |\tau^z=-1\rangle, |T_0\rangle \rightarrow |\tau^z=+1\rangle$). It has been proposed to use two pseudo-spin states such as $|S\rangle$ and $|T_0\rangle$ as a logical qubit.³¹

We assume a time–dependent exchange of the form

$$J = J(t) = J_0 + i\cos(\omega t). \tag{2}$$

The operator δh^z commutes with the Hamiltonian at all times. Thus, if the nuclear spin system is in an

eigenstate $|n\rangle$ of δh^z with $\delta h^z |n\rangle = \delta h_n^z |n\rangle$, we have $H |\psi\rangle = H_n |\psi_e\rangle \otimes |n\rangle$, where in H_n the operator δh^z has been replaced by δh_n^z and $|\psi_e\rangle$ is the electron part of the eigenstate. In order to bring H_n to a form that is very similar to the standard ESR (electron spin resonance) Hamiltonian³² $(H_{ESR} = -\frac{1}{2}\epsilon_z\sigma_z - \frac{1}{2}\Delta_x\cos(\omega t)\sigma_x)$ we perform a unitary transformation $U_1 = \exp(-i\frac{\pi}{4}\tau^y)$ which is just a rotation about the y-axis in a Blochsphere picture. Also introducing $\Omega_n = 2(\delta h_n^z + \delta b^z)$, the above Hamiltonian becomes

$$\tilde{H}_n = U_1 H_n U_1^{\dagger} = \frac{J_0}{2} \tau^x + \frac{j}{2} \cos(\omega t) \tau^x - \frac{1}{2} \Omega_n \tau^z.$$
 (3)

The Pauli matrices are now given in the new basis of $|\downarrow\uparrow\rangle = |\tau^z = 1\rangle$ and $|\uparrow\downarrow\rangle = |\tau^z = -1\rangle$. For $J_0 = 0$ this is just the standard ESR Hamiltonian. We have evaluated pseudo–spin dynamics under this Hamiltonian in a rotating wave approximation close to resonance for $j \ll \Omega_n$. When we treat the J_0 –term as a perturbation and calculate the transition probability between unperturbed eigenstates of the Hamiltonian we find that it is proportional to J_0^2/Ω_n^2 and we may thus neglect this term close to resonance and if $J_0 \ll \Omega_n$. Initializing the two-electron system in the state $|\downarrow\uparrow\rangle = |\tau^z = 1\rangle$ (which can be done as proposed in Sec. IV) we obtain for the expectation value of $\tau^z(t)$:

$$\langle \tau^{z}(t) \rangle_{n} = \langle n | \otimes \langle \downarrow \uparrow | \tau^{z}(t) | \downarrow \uparrow \rangle \otimes | n \rangle$$

$$= \frac{(\Omega_{n} - \omega)^{2} + (j/2)^{2} \cos(\omega' t)}{(\Omega_{n} - \omega)^{2} + (j/2)^{2}}, \tag{4}$$

$$\omega' = 2\sqrt{(\Omega_n - \omega)^2 + (j/2)^2},\tag{5}$$

$$j \ll \Omega_n, \ J_0 \ll \Omega_n, \ |\Omega_n - \omega| \ll \Omega_n.$$
 (6)

For $\omega = \Omega_n$ the system undergoes coherent Rabi oscillations between the states $|\downarrow\uparrow\rangle$ and $|\uparrow\downarrow\rangle$ with a frequency of j. Averaged over time, the expectation value of τ^z is

$$\langle \langle \tau^z \rangle \rangle_n = \lim_{T \to \infty} \frac{1}{T} \int_0^T \langle \tau^z(t) \rangle_n dt = \frac{(\Omega_n - \omega)^2}{(\Omega_n - \omega)^2 + (j/2)^2}.$$
(7)

In order to measure the time–averaged value $\langle\langle \tau^z \rangle\rangle_n$ the measurement time must be much larger than the period of Rabi oscillations ($\sim 1/j$ on resonance). $1 - \langle\langle \tau^z \rangle\rangle_n$ has a Lorentzian line shape with a full width at half maximum (FWHM) of j. Most importantly, the resonance frequency depends on the nuclear spin eigenstate through $\Omega_n = 2(\delta h_n^z + \delta b^z)$ and thus a measurement of the resonance will determine δh_n^z .

A. Superposition of nuclear spin eigenstates

We now investigate how the resonance changes if we consider the nuclear spin system to be in a more general state.

At t = 0 we fix the electron system in the state $|\downarrow\uparrow\rangle$ while the nuclear spin system is in an arbitrary pure state:³³ $\rho(0) = \rho_e(0) \otimes \rho_I(0)$ with

$$\rho_e(0) = |\downarrow\uparrow\rangle\langle\downarrow\uparrow|, \tag{8}$$

$$\rho_I(0) = |\psi_I\rangle \langle \psi_I|; |\psi_I\rangle = \sum_n a_n |n\rangle, \qquad (9)$$

where the a_n satisfy the normalization condition $\sum_n |a_n|^2 = 1$. Here, $\rho_I(n) = |a_n|^2$ are the diagonal elements of the nuclear–spin density operator. The Hamiltonian H_0 commutes with δh^z and thus we find

$$\overline{\langle \tau^z(t) \rangle} = \sum_n \rho_I(n) \langle \tau^z(t) \rangle_n, \tag{10}$$

which defines the overbar.

We assume that for a large number of nuclear spins $N \gg 1$ which are in a superposition of δh^z -eigenstates $|n\rangle$, $\rho_I(n)$ describes a continuous Gaussian distribution of δh^z_n values, with mean $\overline{\delta h^z}$ and variance $\sigma^2 = \overline{\left(\delta h^z - \overline{\delta h^z}\right)^2}$. In the limit of large N the approach to a Gaussian distribution for a sufficiently randomized nuclear system is guaranteed by the central limit theorem.¹⁷ We perform the continuum limit according to

$$\sum_{n} \rho_{I}(n) f(n) \rightarrow \int dx P_{\sigma; \overline{x}}(x) f(x), \qquad (11)$$

$$P_{\sigma;\overline{x}}(x) = \frac{1}{\sqrt{2\pi}\sigma} \exp\left(-\frac{(x-\overline{x})^2}{2\sigma^2}\right), (12)$$

where $x = \delta h_n^z$, $\overline{x} = \overline{\delta h^z}$ and $\sigma^2 = \overline{x^2} - \overline{x}^2$. The only effect of δb^z is to shift the mean value of the Overhauser field inhomogeneity to $x_0 = \overline{x} + \delta b^z$, whereas the width is left unchanged: $\sigma_0 = \sigma$. According to this description we obtain

$$\overline{\langle \tau^z(t) \rangle} = \int_{-\infty}^{\infty} dx P_{\sigma_0;x_0}(x) \left(f(x) + g(x,t) \right), \quad (13)$$

$$f(x) = \frac{(2x - \omega)^2}{(2x - \omega)^2 + (j/2)^2},$$
(14)

$$g(x,t) = \frac{(j/2)^2 \cos\left(2\sqrt{(2x-\omega)^2 + (j/2)^2}t\right)}{(2x-\omega)^2 + (j/2)^2}.(15)$$

The second term vanishes when it is averaged over time and we find

$$1 - \overline{\langle \langle \tau^z \rangle \rangle} = \frac{1}{2\sigma_0 \sqrt{2\pi}} \int_{-\infty}^{\infty} dx \exp\left(-\frac{(x - 2x_0)^2}{8\sigma_0^2}\right) \frac{(j/2)^2}{(x - \omega)^2 + (j/2)^2}.$$
 (16)

This integral is the well-known Voigt function,³⁴ and the resulting lineshape is the so-called "Voigt profile". The Voigt function may be expressed as $(\tilde{\omega} = j + 4ix_0 - 2i\omega)$

$$\overline{\langle\langle\langle\tau^z\rangle\rangle\rangle} = 1 - \frac{j}{4\sigma_0} \sqrt{\frac{\pi}{2}} \operatorname{Re} \left[\exp\left(\frac{\tilde{\omega}^2}{32\sigma_0^2}\right) \operatorname{erfc}\left(\frac{\tilde{\omega}}{4\sqrt{2}\sigma_0}\right) \right], \tag{17}$$

where $\operatorname{erfc}(z)$ is the complementary error function. In the regime where $\sigma_0 \ll j$ we may approximate the Lorentzian in the convolution by its value at $x = 2x_0$ and obtain

$$\overline{\langle\langle \tau^z \rangle\rangle} \approx \frac{(2x_0 - \omega)^2}{(2x_0 - \omega)^2 + (j/2)^2}; \quad \sigma_0 \ll j.$$
 (18)

In this case the resulting resonance has the same FWHM as the Lorentzian, viz. j. On the other hand, if $\sigma_0 \gg j$, we may approximate the Gaussian with its value at $x = \omega$

and thus obtain

$$\overline{\langle\langle\langle\tau^z\rangle\rangle} \approx 1 - \frac{j}{4\sigma_0} \sqrt{\frac{\pi}{2}} \exp\left(-\frac{(2x_0 - \omega)^2}{8\sigma_0^2}\right); \quad \sigma_0 \gg j.$$
 (19)

In this regime the width is twice the width of the Gaussian distribution of the nuclear spin states. In order to make a statement about the width of the Voigt profile in general we look at the peak–to–peak separation Δ_V of the first derivative of the Voigt profile. For a Gaussian with a standard deviation of σ_0 we find $\Delta_G=2\sigma_0$ for the peak–to–peak separation of the derivative and for a Lorentzian with FWHM of j we have $\Delta_L=j/\sqrt{3}$. A Padé approximant for Δ_V in terms of Δ_L and Δ_G yields 35

$$\Delta_V = \frac{\Delta_G^2 + a_1 \Delta_G \Delta_L + a_2 \Delta_L^2}{\Delta_G + a_2 \Delta_L} \tag{20}$$

where $a_1 = 0.9085$, $a_2 = 0.4621$. This approximation is accurate to better than $0.01\Delta_V$ for all values

of Δ_L, Δ_G .³⁵ A similar formula may also be given for the half width at half maximum (HWHM) of the Voigt profile.³⁶

B. State narrowing

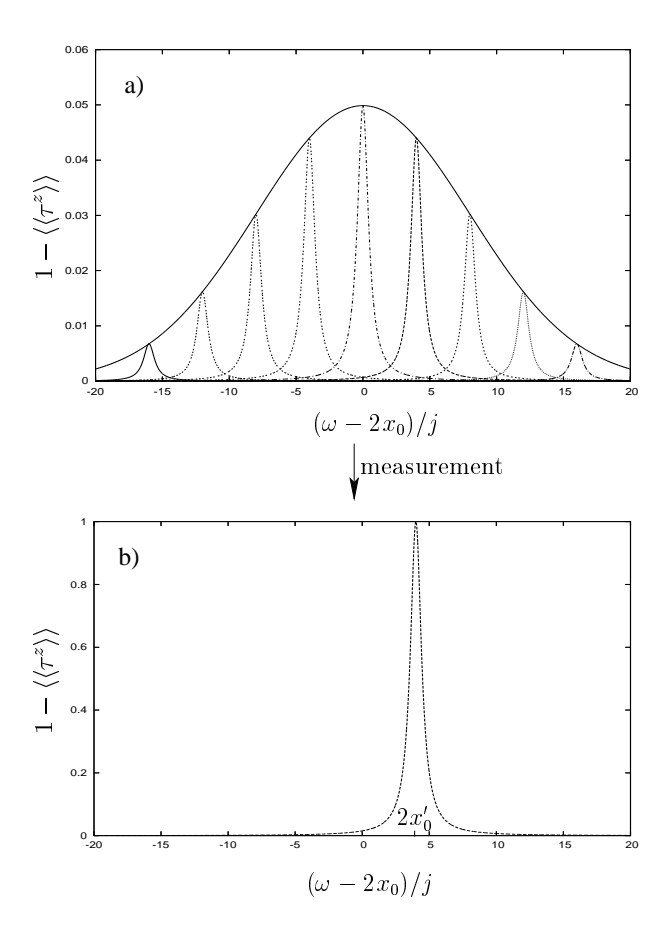


FIG. 1: a) This figure illustrates the projection obtained through an ideal measurement of the Rabi resonance. All the different Lorentzian resonances corresponding to different nuclear spin eigenstates add up to a Gaussian lineshape. b) Through a perfect measurement of the Rabi resonance, which involves many measurements of τ^z , the superposition collapses and we are left with one single Lorentzian centered around $2x'_0 = \Omega_n$ which in general is different from $2x_0$.

The Rabi resonance in the case where the nuclear spin system is in an eigenstate $|n\rangle$ is centered around $\Omega_n = 2(\delta h_n^z + \delta b^z)$ and thus a measurement of this resonance is also a measurement of δh_n^z . In the case of a superposition of nuclear spin eigenstates the resonance is a superposition of many Lorentzian resonances each centered around a different Ω_n . A measurement of the resonance leads to a projection of this superposition (in the ideal case to a subspace with fixed eigenvalue δh_n^z) and thus to a narrowing of the nuclear spin distribution. We now use the above results to explain how the mea-

surement of the resonance leads to narrowing.

We assume the nuclear spin system to be in a fixed pure state during the course of the measurement, in particular δh^z must be static during the measurement procedure. We expect δh^z to vary on the time scale of nuclear spin diffusion out of the dot. However, there may be other sources of nuclear spin dynamics (see e.g. Appendix A). In a GaAs double quantum dot containing $N=10^6$ nuclei we have $\sigma_0=A/\sqrt{N}\sim 0.1\mu \text{eV}$. The amplitude j of the oscillating exchange coupling J(t) must satisfy $j \ll \sigma_0$ to narrow the nuclear spin state beyond its natural linewidth σ_0 . This regime should be accessible with currently available experimental apparatus.⁹ The resonance that results from the Gaussian distributed superposition of nuclear spin eigenstates has a width of $\sim 2\sigma_0$ in the regime considered and is centered around $2x_0$. This can be seen as the superposition of Lorentzian lineshapes which are the resonances resulting from many nuclear spin eigenstates $|n\rangle$ making up the Gaussian distribution of nuclear spin eigenstates. Each Lorentzian is weighted according to the amplitude of the corresponding nuclear spin eigenstate in the Gaussian-distributed superposition (see Fig. 1 a).

Solving Eq. (20) for Δ_G and taking the positive solution yields for the standard deviation of the nuclear spin distribution after the measurement

$$\sigma_0' = \frac{1}{4} (\Delta_V - a_1 \Delta_L + \sqrt{(\Delta_V - a_1 \Delta_L)^2 + 4a_2 \Delta_L (\Delta_V - \Delta_L)}) (21)$$

Thus, σ_0' depends on $\Delta_L = j/\sqrt{3}$ and the Δ_V measured for the resonance. If, in an experiment the Δ_V measured is small enough, we have $\sigma_0' < \sigma_0$, i.e., we have narrowed the nuclear spin state.

In the ideal case where the resonance is measured with perfect accuracy (unit fidelity) we obtain a Lorentzian lineshape which is centered around $2x'_0 = \Omega_n = 2(\delta h_n^z +$ δb^z) and thus δh_n^z is determined (see Fig. 1 b). According to the postulates of quantum mechanics, it follows then that after the measurement the nuclear system must be in one of the degenerate eigenstates $|n\rangle$ belonging to the measured eigenvalue δh_n^z . This case, where the measured Voigt profile is the Lorentzian resulting from a fixed eigenvalue δh_n^z , corresponds to perfect narrowing, i.e. $\sigma'_0 = 0$. Of course in a realistic measurement only the width is measured and not with perfect accuracy, but with some error. This error comes from the fact that a measurement of the resonance consists of many measurements of τ^z which are only known up to some uncertainty. Further, we may only measure a finite number of expectation values for τ^z to which the lineshape must be fitted. This leads to an uncertainty in the width Δ_V of the Voigt profile which, together with uncertainty in j, contributes to the uncertainty of σ'_0 . The level of narrowing obtained therefore depends on the accuracy of the measurement which is limited by the number of pseudo-spin measurements that can be performed within the nuclear

spin diffusion time. The success of the narrowing procedure can be tested by a subsequent measurement of the decoherence time of the pseudo-spin correlators (see Sec. III). We also note that if the hyperfine field were classical with some uncertainty (dynamically produced e.g. by fluctuations in time) then the narrowing procedure described here would not reduce that uncertainty since a classical field is not affected by a measurement.

The general requirements on the parameters of the system for this scheme to narrow the nuclear spin state are

$$x_0 \gtrsim j, J_0; \quad \sigma_0 \gtrsim j.$$
 (22)

We note that, unlike in standard ESR, power absorption is not measured here, but instead the expectation value of the pseudo-spin, for instance via a quantum point contact (QPC) nearby one quantum dot. For a detailed description of the measurement process via such a QPC we refer the interested reader to Ref. 37.

III. CORRELATION FUNCTIONS IN THE $S^z=0$ SUBSPACE

In this section we investigate the Hamiltonian H_0 of Eq. (1) with static exchange coupling J. Using this Hamiltonian we wish to calculate correlation functions for several observables in the subspace of zero total spin in the z-direction. In our previous work¹⁸ we calculated the time evolution of a particular correlator involving the states $|S\rangle$ and $|T_0\rangle$. However, there are four additional independent correlators involving the x and y components of pseudo-spin which require a separate calculation. Quite surprisingly, it will turn out that these correlators have different decay behavior in time. The correlators we calculate here show the decoherence properties of the pseudo-spin states under the influence of the hyperfine interaction. There may be additional sources of decoherence which we do not consider here, such as orbital dephasing, corrections to the effective Hamiltonian, ¹⁸ the coupling of the QPC to the dot spins, 38 etc. The results of this section will help to give requirements on the parameters of the system in order to initialize in the state $|\uparrow\downarrow\rangle$ and to assess the fidelity of a $\sqrt{\text{SWAP}}$ operation with static J (see Sec. IV).

Diagonalizing H_0 gives the following eigenvalues and eigenvectors

$$E_n^{\pm} = \frac{J}{2} \pm \frac{1}{2} \sqrt{J^2 + \Omega_n^2},$$
 (23)

$$\left| E_n^{\pm} \right\rangle = \frac{\left(\Omega_n / 2 \right) \left| S \right\rangle + E_n^{\pm} \left| T_0 \right\rangle}{\sqrt{\left(E_n^{\pm} \right)^2 + \left(\Omega_n / 2 \right)^2}} \otimes \left| n \right\rangle, \tag{24}$$

where again $|n\rangle$ is an eigenstate of the operator δh^z with $\delta h^z |n\rangle = \delta h_n^z |n\rangle$. At t=0 we fix the electron system in an arbitrary superposition of $|T_0\rangle$ and $|S\rangle$

$$|\psi_e(t=0)\rangle = |A\rangle; |A\rangle = \cos\frac{\theta_A}{2}|S\rangle + e^{i\varphi_A}\sin\frac{\theta_A}{2}|T_0\rangle.$$
 (25)

The nuclear spin system is again in a general pure state³³ (see Sec. II A). As will be shown in Sec. IV, it is possible, in principle, to initialize to an arbitrary state in the subspace spanned by $|T_0\rangle$ and $|S\rangle$. The probability to find the electron spins in a state $|B\rangle$ at t>0 is given by the correlation function:

$$C_{BA}(t) = \sum_{n} \rho_{I}(n) \left| \langle n | \otimes \langle B | e^{-iH_{0}t} | A \rangle \otimes | n \rangle \right|^{2}, \quad (26)$$

where $\rho_I(n) = |a_n|^2$. The correlation function has the following symmetry: $C_{BA}(t) = C_{AB}(-t)$, and if $|B\rangle$ and $|D\rangle$ are orthogonal states we have $C_{BA}(t) = 1 - C_{DA}(t)$. Further, we may decompose $C_{BA}(t)$ into the sum of a time-independent term $\overline{C_{BA}^n}$ and an interference term $C_{BA}^{\text{int}}(t)$:

$$C_{BA}(t) = \overline{C_{BA}^n} + C_{BA}^{\text{int}}(t), \tag{27}$$

where the overbar is defined in Eq. (10).

We have further $C_{BA}^n = C_{BA}(\delta h_n^z) = C_{BA}(x)$. Performing the continuum limit as described in Eq. (11) we obtain for the correlation function

$$C_{BA}(t) = \int_{-\infty}^{\infty} dx P_{\sigma_0; x_0}(x) \left(C_{BA}(x) + C_{BA}^{\text{int}}(x, t) \right) (28)$$
$$= C_{BA}^{\infty} + C_{BA}^{\text{int}}(t). \tag{29}$$

We have calculated correlation functions for the following states: $|S\rangle \to |\tau^z=-1\rangle$, $|T_0\rangle \to |\tau^z=+1\rangle$, $|X\rangle \to |\tau^x=+1\rangle = \frac{1}{\sqrt{2}}\left(|T_0\rangle + |S\rangle\right)$, $|Y\rangle \to |\tau^y=+1\rangle = \frac{1}{\sqrt{2}}\left(|T_0\rangle + i|S\rangle\right)$. The frequency in the interference term is always given by $s(x)=\sqrt{J^2+4x^2}$. In Table I we list the integrands according to the notation in Eq. (28).

$C_{BA}(t)$	$C_{BA}(x)$	$C_{BA}^{\mathrm{int}}(x,t)$
$C_{T_0S}(t)$	$\frac{2x^2}{s(x)^2}$	$-\frac{2x^2}{s(x)^2}\cos(s(x)t)$
$C_{T_0X}(t)$	$\frac{1}{2} + \frac{Jx}{s(x)^2}$	$-\frac{Jx}{s(x)^2}\cos(s(x)t)$
$C_{T_0Y}(t)$	$\frac{1}{2}$	$\frac{x}{s(x)}\sin(s(x)t)$
$C_{YX}(t)$	$\frac{1}{2}$	$\frac{J}{2s(x)}\sin(s(x)t)$
$C_{YY}(t)$	$\frac{1}{2}$	$\frac{1}{2}\cos(s(x)t)$
$C_{XX}(t)$	$\frac{1}{2} + \frac{2x^2}{s(x)^2}$	$\left(\frac{1}{2} - \frac{2x^2}{s(x)^2}\right)\cos(s(x)t)$

TABLE I: Functions $C_{BA}(x)$ and $C_{BA}^{\text{int}}(x,t)$ according to the notation of Eq. (28) for different correlators (with $s(x) = \sqrt{J^2 + 4x^2}$). $C_{XX}(t)$ is a linear combination of other correlators.

We see that $C_{XX}(t)$ is a linear combination of other correlators: $C_{XX}(t) = C_{YY}(t) + C_{T_0S}(t)$. For C_{T_0X} and C_{T_0Y} the interference term is an odd function in x. Thus the time dependence vanishes for $x_0 = 0$ and we have

 $C_{T_0X} = C_{T_0Y} = 1/2$ for all t. In general, the integral in Eq. (28) is difficult to solve exactly. Thus, we concentrate on several interesting limits. We illustrate this for the case of $C_{YX}(t)$ and give results for the other correlators. We have

$$C_{YX}(t) = \frac{1}{2} + \operatorname{Im} \left[\tilde{C}_{YX}^{\text{int}} \right],$$
 (30)

$$\tilde{C}_{YX}^{\text{int}} = \int_{-\infty}^{\infty} P_{\sigma_0; x_0}(x) \frac{J}{2s(x)} e^{is(x)t}.$$
 (31)

In the regime of $|x_0|\gg\sigma_0$ the main contribution to the integral comes from a narrow region around x_0 and we may approximate $\frac{J}{2s(x)}\approx\frac{J}{2\omega_0}$ where $\omega_0=s(x_0)$ and in the frequency term $s(x)\approx\omega_0+\frac{4x_0}{\omega_0}(x-x_0)+\dots$. For this to be a good approximation, we require $\frac{2J^2}{w_0^3}(x-x_0)^2t\ll 1$. We use $(x-x_0)^2\approx\sigma_0^2$ and thus obtain for the correlator and the range of validity in this limit

$$C_{YX}^{\text{int}}(t) = \frac{J}{2\omega_0} e^{-\frac{1}{2} \left(\frac{t}{t_0''}\right)^2} \sin(\omega_0 t),$$
 (32)

$$t_0'' = \frac{\omega_0}{4|x_0|\sigma_0}, \ \omega_0 = \sqrt{J^2 + 4x_0^2}, \ (33)$$

$$|x_0| \gg \sigma_0, \ t \ll \frac{(J^2 + 4x_0^2)^{3/2}}{2J^2\sigma_0^2}.$$
 (34)

The results for the other correlators are (with the same range of validity)

$$C_{T_0S}^{\text{int}}(t) = -\frac{2x_0^2}{\omega_0^2} e^{-\frac{1}{2} \left(\frac{t}{t_0^{\prime\prime\prime}}\right)^2} \cos(\omega_0 t),$$
 (35)

$$C_{T_0X}^{\text{int}}(t) = -\frac{Jx_0}{\omega_0^2} e^{-\frac{1}{2} \left(\frac{t}{t_0^{\prime\prime}}\right)^2} \cos(\omega_0 t),$$
 (36)

$$C_{T_0Y}^{\text{int}}(t) = \frac{x_0}{\omega_0} e^{-\frac{1}{2} \left(\frac{t}{t_0''}\right)^2} \sin(\omega_0 t),$$
 (37)

$$C_{YY}^{\text{int}}(t) = \frac{1}{2}e^{-\frac{1}{2}\left(\frac{t}{t_0^{\prime\prime\prime}}\right)^2}\cos(\omega_0 t).$$
 (38)

In this limit we obtain a Gaussian decay for all correlators on a time scale $t_0'' = \frac{\omega_0}{4|x_0|\sigma_0}$ which grows with the absolute value of the exchange coupling |J| and with $1/\sigma_0$. The long–time saturation value is 1/2 for C_{YX} . For some of the other correlators we find non–trivial parameter–dependent saturation values. In the limit of $|x_0| \gg \sigma_0$ we obtain these correlators by the same approximation as for the interference term, i.e. we set $C_{BA}(x) = C_{BA}(x_0)$ and obtain

$$C_{T_0S}^{\infty} = \frac{2x_0^2}{J^2 + 4x_0^2},\tag{39}$$

$$C_{T_0X}^{\infty} = \frac{1}{2} + \frac{Jx_0}{J^2 + 4x_0^2},\tag{40}$$

$$C_{T_0Y}^{\infty} = C_{YX}^{\infty} = C_{YY}^{\infty} = \frac{1}{2}; |x_0| \gg \sigma_0.$$
 (41)
For large J the saturation value is quadratic in x_0/J for

For large J the saturation value is quadratic in x_0/J for C_{T_0S} and linear for C_{T_0X} . The saturation value for C_{T_0S} goes to zero for $|J| \gg |x_0|$ and for C_{T_0X} approaches 1/2. $C_{T_0X}^{\infty}$ reaches extrema equal to $\frac{1}{2} + \frac{1}{4} \text{sign}(Jx_0)$ for $|J| = 2|x_0|$.

Next we consider Eq. (28) for $|J| \gg \max(|x_0|, \sigma_0)$ and find

$$s(x) = \sqrt{J^2 + 4x^2} \approx |J| + \frac{2x^2}{|J|},$$
 (42)

$$\frac{J}{2s(x)} = \frac{J}{2\sqrt{J^2 + 4x^2}} \approx \text{sign}(J) \left(\frac{1}{2} - \frac{x^2}{J^2}\right).$$
 (43)

For Eq. (42) we have the additional requirement that $t \ll \frac{|J|^3}{2\max(x_0^4, \sigma_0^4)}$. Under these approximations we find the following result:

$$\tilde{C}_{YX}^{\text{int}}(t) = \operatorname{sign}(J) \left(\frac{1}{2} \xi(t) - \frac{\sigma_0^2}{J^2} \xi^3(t) - \frac{x_0^2}{J^2} \xi^5(t) \right) \exp\left(i|J|t - \frac{x_0^2}{2\sigma_0^2} \left(1 - \xi^2(t)\right)\right), \tag{44}$$

$$\xi(t) = \left(1 - i\frac{t}{t_0'}\right)^{-1/2}, \ t_0' = \frac{|J|}{4\sigma_0^2}, \ |J| \gg \max(|x_0|, \sigma_0), \ t \ll \frac{|J|^3}{2\max(x_0^4, \sigma_0^4)}.$$
 (45)

At short times we expand $\xi^2(t) \sim 1 + i \frac{t}{t_0'} - \left(\frac{t}{t_0'}\right)^2$. Keeping only lowest order in t/t_0' in the prefactor and second

order in the frequency term we obtain

$$C_{YX}^{\text{int}}(t) = \operatorname{sign}(J) \frac{1}{2} e^{-\frac{1}{2} \left(\frac{t}{t_0'}\right)^2} \sin(\omega_0' t), \qquad (46)$$

$$t_0'' \approx \frac{|J|}{4|x_0|\sigma_0}, \quad \omega_0' = |J| + \frac{2(x_0^2 + \sigma_0^2)}{|J|} (47)$$

$$t \ll t_0' = \frac{|J|}{4\sigma_0^2}, \ |J| \gg \max(|x_0|, \sigma_0).$$
 (48)

The $|x_0| \gg \sigma_0$ limit of this result agrees with the $|J| \gg |x_0|$ limit of Eq. (32). Again, we have a Gaussian decay on the same time scale t_0'' as in Eq. (32) $(\omega_0 = \sqrt{J^2 + 4x_0^2} \sim |J| \text{ for } |J| \gg |x_0|)$. One interesting feature of this correlator is the fact that there is a change of phase by π when the sign of the exchange coupling J changes. This feature offers the possibility of measuring J even for small values of J through a measurement of this correlator. We also list the other correlators in this regime:

$$C_{T_0S}^{\text{int}}(t) = -\frac{2(x_0^2 + \sigma_0^2)}{J^2} e^{-\frac{1}{2} \left(\frac{t}{t_0^{\prime\prime}}\right)^2} \cos(\omega_0^{\prime} t), \quad (49)$$

$$C_{T_0X}^{\text{int}}(t) = -\frac{x_0}{J}e^{-\frac{1}{2}\left(\frac{t}{t_0'}\right)^2}\cos(\omega_0't),$$
 (50)

$$C_{T_0Y}^{\text{int}}(t) = \frac{x_0}{|J|} e^{-\frac{1}{2} \left(\frac{t}{t_0^{\prime\prime}}\right)^2} \sin(\omega_0^{\prime} t),$$
 (51)

$$C_{YY}^{\text{int}}(t) = \frac{1}{2}e^{-\frac{1}{2}\left(\frac{t}{t_0''}\right)^2}\cos(\omega_0't).$$
 (52)

Finally, we are also interested in the behavior for large t. Thus, we expand Eq. (44) for large times $\xi(t\gg t_0')\sim e^{i\pi/4}\sqrt{t_0'/t}$ and obtain

$$C_{YX}^{\text{int}}(t) \sim \text{sign}(J)e^{-\frac{x_0^2}{2\sigma_0^2}} \frac{\sqrt{|J|}\sin(|J|t + \frac{\pi}{4})}{4\sigma_0 t^{\frac{1}{2}}},$$
 (53)

$$t \gg t_0' = \frac{|J|}{4\sigma_0^2}, |J| \gg \max(|x_0|, \sigma_0).$$
 (54)

For the other correlators we find

$$C_{T_0S}^{\text{int}}(t) \sim e^{-\frac{x_0^2}{2\sigma_0^2}} \frac{\cos(|J|t + \frac{3\pi}{4})}{4\sigma_0\sqrt{|J|}t^{\frac{3}{2}}},$$
 (55)

$$C_{T_0X}^{\text{int}}(t) \sim -\text{sign}(J)e^{-\frac{x_0^2}{2\sigma_0^2}} \frac{x_0\sqrt{|J|}\cos(|J|t+\frac{3\pi}{4})}{8\sigma_0^3t^{\frac{3}{2}}}$$
(56)

$$C_{T_0Y}^{\text{int}}(t) \sim e^{-\frac{x_0^2}{2\sigma_0^2}} \frac{x_0\sqrt{|J|}\sin(|J|t + \frac{3\pi}{4})}{8\sigma_0^3 t^{\frac{3}{2}}},$$
 (57)

$$C_{YY}^{\text{int}}(t) \sim e^{-\frac{x_0^2}{2\sigma_0^2}} \frac{\sqrt{|J|}\cos(|J|t + \frac{\pi}{4})}{4\sigma_0 t^{\frac{1}{2}}}.$$
 (58)

(59)

Thus, the transverse components of the pseudo-spin have a slower decay ($\sim t^{-1/2}$) than the longitudinal component ($\sim t^{-3/2}$). This results from the fact that the Hamiltonian only has fluctuations in one direction.

IV. IMPLEMENTATION OF $\sqrt{\text{SWAP}}$

In this section we show how the $\sqrt{\text{SWAP}}$ gate may be implemented using the Hamiltonian in Eq. (1). This is important since $\sqrt{\text{SWAP}}$ and single-qubit operations can be used to perform the quantum XOR gate (CNOT)

which, in combination with single–qubit operations, is sufficient for universal quantum computation. ^{1,39} In Ref. 9 implementation of $\sqrt{\text{SWAP}}$ has been demonstrated. However, in these experiments there was a contrast reduction of $\sim 40\%$. Here we show that in some regime near–unit fidelity can be obtained.

The Hamiltonian of Eq. (1) induces unitary time evolution on the states of the system: $|\psi(t)\rangle = U(t) |\psi(0)\rangle$ with $U(t) = T \exp(-i \int_0^t H(t') dt')$. We assume that J and x_0 can be switched on a time scale that is much shorter than the time required for the gate operation and thus the time evolution operator at time τ_s has the form

$$U_s = \exp\left(-i\tau_s H\right). \tag{60}$$

In a Bloch–sphere picture⁹ this operator induces a rotation about an axis in the plane spanned by eigenstates of τ^x and τ^z , $|X\rangle = |\uparrow\downarrow\rangle$ and $|S\rangle = (|\uparrow\downarrow\rangle - |\downarrow\uparrow\rangle)/\sqrt{2}$. Through such an operation any state may be rotated into any other state on the Bloch sphere. Thus, it is possible to rotate from $|S\rangle$ to any initial state in the subspace of $S^z = 0$ by a single operation. This is important since initialization to the singlet is feasible by preparing a ground-state singlet with both electrons on the same dot and then changing the bias. 9 We now explicitly show that initialization to the state $|X\rangle$ is possible. The scheme we propose here is different from the one used in Ref. 9, where adiabatic passage from the singlet to the $\uparrow\downarrow\rangle$ -state is used. Our scheme requires control of x_0 . We assume the system to be in the singlet state $|S\rangle$ at t=0 and then switch J and x_0 such that $J=-2x_0$ and $|x_0| \gg \sigma_0$. Since $C_{XS}(t) = C_{SX}(-t) = 1 - C_{T_0X}(-t)$ we have, for the above choice of parameters, according to Eq. (36):

$$C_{XS}(t) = \frac{1}{2} + \frac{1}{4} \left(1 - \cos(\sqrt{2}|J|t) \right) e^{-\frac{1}{2} \left(\frac{t}{t_0''}\right)^2}, (61)$$

$$J = -2x_0, \ |x_0| \gg \sigma_0, \tag{62}$$

$$t_0'' = \frac{1}{\sqrt{2}\sigma_0}, \ t \ll \frac{(J^2 + 4x_0^2)^{3/2}}{2J^2x_0^2}. \tag{63}$$

This correlator reaches its maximum for $\sqrt{2}|J|t=\pi$, i.e., at $\tau_s=\frac{\pi}{\sqrt{2}|J|}$. The time scale for the Gaussian decay is $t''=\frac{1}{\sqrt{2}\sigma_0}$. To approach unit fidelity we therefore require $|J|\gg\sigma_0$, which is the case in the range of validity of the above correlator since $|x_0|\gg\sigma_0$ and J and x_0 are of the same order. At $t=\tau_s$ we switch J to zero and since $|X\rangle\otimes|n\rangle$ is an eigenstate of the remaining Hamiltonian the system remains in this product state, untouched by decoherence induced via the nuclear spins. This scheme thus provides a way to initialize the double quantum dot system to the state $|X\rangle=\frac{1}{\sqrt{2}}(|T_0\rangle+|S\rangle)=|\uparrow\downarrow\rangle$, where arrows denote the z-component of the electron spin in each dot. In the same way, it is also possible to initialize in the state $|-X\rangle=|\tau^x=-1\rangle=\frac{1}{\sqrt{2}}(|T_0\rangle-|S\rangle)=|\downarrow\uparrow\rangle$ by switching to $J=2x_0$.

Next we show that it is possible to perform a SWAP operation with the Hamiltonian H_0 . The SWAP operation acts on the basis of the two-electron system as: $|\downarrow\downarrow\rangle \rightarrow |\downarrow\downarrow\rangle, |\downarrow\uparrow\rangle \rightarrow |\uparrow\downarrow\rangle, |\uparrow\downarrow\rangle \rightarrow |\downarrow\uparrow\rangle, |\uparrow\uparrow\rangle \rightarrow |\uparrow\uparrow\rangle.$ The SWAP is an operation that acts only on the subspace of $S^z = 0$ and leaves the states $|\uparrow\uparrow\rangle$ and $|\downarrow\downarrow\rangle$ unchanged. In the system we consider this is naturally implemented through the large Zeeman splitting that separates $|\uparrow\uparrow\rangle$ and $|\downarrow\downarrow\rangle$ from the singlet and the $S^z=0$ triplet. In order to accomplish the SWAP in the $S^z = 0$ subspace we consider the regime of $|J| \gg \max(x_0, \sigma_0)$. The correlator $C_{-X,X}(t)$ gives the probability of being in the state $|-X\rangle = |\downarrow\uparrow\rangle$ for a system initialized in $|X\rangle = |\uparrow\downarrow\rangle$. Due to the symmetry relations for the correlation functions we have $C_{-X,X}(t) = 1 - C_{XX}(t) = 1 - C_{YY}(t) - C_{T_0S}(t)$ and thus find (using Eqs. (49), (52) and neglecting terms of order $(\sigma_0^2 + x_0^2)/J^2$,

$$C_{-X,X}(t) = 1 - C_{XX}(t) \approx \frac{1}{2} - \frac{1}{2}e^{-\frac{1}{2}\left(\frac{t}{t_0^{\prime\prime}}\right)^2}\cos(|J|t),$$
(64)

$$t_0'' = \frac{1}{\sqrt{2}\sigma_0}, \ |J| \gg \max(x_0, \sigma_0), \ t \ll t_0' = \frac{|J|}{4\sigma_0^2}.$$
 (65)

We obtain the maximum value for this correlator for $\tau_s=\frac{\pi}{|J|}$. The Gaussian has a decay time of $t''=\frac{|J|}{4\sigma_0|x_0|}$, so for $x_0\to 0$ the Gaussian decay is negligible and we obtain unit fidelity for this SWAP operation $|\uparrow\downarrow\rangle\to|\downarrow\uparrow\rangle$ up to a global phase factor (which is not visible in the correlator).

From the SWAP operation it is only a small step towards the $\sqrt{\text{SWAP}}$ which we obtain when we let the system evolve with the same parameter values but for only half the time. Starting in the state $|X\rangle$ we obtain $|Y\rangle$ after applying a $\sqrt{\text{SWAP}}$. For large |J| we find for the correlator C_{YX} in the limit $x_0 \to 0$

$$C_{YX}(t) = \frac{1}{2} + \operatorname{sign}(J) \frac{1}{2} e^{-\frac{1}{2} \left(\frac{t}{t_0''}\right)^2} \sin(|J|t), \quad (66)$$

$$t_0'' = \frac{1}{\sqrt{2}\sigma_0}, \ |J| \gg \max(x_0, \sigma_0), \ t \ll t_0' = \frac{|J|}{4\sigma_0^2}.(67)$$

Here again the time scale of the Gaussian decay is $\frac{|J|}{4\sigma_0|x_0|}$ and approaches infinity for $x_0 \to 0$. The time during which we have to operate with these values of the parameters J and x_0 is now $t_g = \frac{\pi}{2|J|}$. Our calculations show that for the time during which J is pulsed high there is a regime in which unit fidelity may be approached. The reduced visibility in the experiment f may be due to several reasons such as reduced visibility in the readout of f or the initialization of f

V. CONCLUSION

We have developed a method that uses the measurement of a Rabi resonance in the quantum dot spin-qubit to narrow the distribution of the nuclear spin states. This method relies on Rabi oscillations induced via an oscillation of the singlet–triplet splitting J in the subspace $S^z=0$ of two electrons in a double quantum dot forming a two–qubit system. Further, we have calculated several correlators in the $S^z=0$ subspace for static J and found that the transverse components of pseudo–spin have a slower decay than the longitudinal one. We have also discussed the implementation and fidelity of the $\sqrt{\text{SWAP}}$ –gate in this system and the initialization to the $|\uparrow\downarrow\rangle,|\downarrow\uparrow\rangle$ states.

Acknowledgments

We thank G. Burkard, M. Duckheim, J. Lehmann, F. H. L. Koppens, D. Stepanenko and, in particular, A. Yacoby for useful discussions. We acknowledge financial support from the Swiss NSF, the NCCR nanoscience, EU NoE MAGMANet, DARPA, ARO, ONR, JST ICORP, and NSERC of Canada.

APPENDIX A: DRIFT IN δh^z

In addition to spin diffusion, driven by the nuclear dipole-dipole interaction, there may also be a change in δh^z due to corrections to the projected effective Hamiltonian considered here (see Ref. 18, Appendix B for details). After tracing out the electron pseudo–spin in state ρ_S , these correction terms give rise to an electron-mediated nuclear spin-spin interaction which, in general, takes the form of an anisotropic (XYZ) Heisenberg interaction

$$H_{nn} = \text{Tr}_S\{\rho_S H\} = \sum_{i,j,\alpha = \{x,y,z\}} J_{ij}^{\alpha} I_i^{\alpha} I_j^{\alpha}.$$
 (A1)

Here, the indices i and j run over all nuclear spin sites.

We use the corrections to leading order in the inverse Zeeman splitting $1/\epsilon_z$ ($\epsilon_z = g\mu_B B$) given in Ref. 18. This gives the typical value of the exchange constants $\left|J_{ij}^{\alpha}\right| \sim A^2/N^2\epsilon_z$. Assuming an unpolarized nuclear spin state, each nuclear spin will therefore precess in an effective mean field generated by all other spins in the dot of typical magnitude

$$h_{\text{eff}} \sim \sqrt{N} \left| J_{ij}^{\alpha} \right| \sim A^2 / N^{\frac{3}{2}} \epsilon_z.$$
 (A2)

This effective field will result in precession of the nuclear spins about an arbitrary angle (and hence, may change the value of δh^z) on a time scale

$$\tau_p \sim N^{\frac{3}{2}} \epsilon_z / A^2 \sim 10^{-2} \,\mathrm{s},$$
 (A3)

where we have assumed $N=10^6$ nuclear spins within the quantum dot, and $\epsilon_z/g\mu_B=A/g\mu_B\simeq 3.5\,\mathrm{T}$ for the time estimate. This is only a worst–case estimate, which neglects the effects, e.g., of a Knight-shift gradient (due to strong confinement of the electron), which may further

weaken the dynamical effect discussed here. We expect the dipolar nuclear spin diffusion time to be the limiting time scale for nuclear spin dynamics, in light of experiments on diffusion near donor impurities in GaAs.²⁷ If the effect giving rise to τ_p in Eq. (A3) were significant, it could be further suppressed by choosing a larger quantum dot size or stronger magnetic field, thus allowing many electron spin measurements on the time scale of variation of δh^z .

- ¹ D. Loss and D. P. DiVincenzo, Phys. Rev. A **57**, 120 (1998).
- ² H.-A. Engel and D. Loss, Science **309**, 586 (2005).
- ³ V. Cerletti, W. A. Coish, O. Gywat, and D. Loss, Nanotechnology 16, 27 (2005).
- ⁴ K. Ono, D. G. Austing, Y. Tokura, and S. Tarucha, Science 297, 1313 (2002).
- ⁵ K. Ono and S. Tarucha, Phys. Rev. Lett. **92**, 256803 (2004).
- ⁶ A. C. Johnson, J. R. Petta, J. M. Taylor, A. Yacoby, M. D. Lukin, C. M. Marcus, M. P. Hanson, and A. C. Gossard, Nature 435, 925 (2005).
- ⁷ T. Hatano, M. Stopa, and S. Tarucha, Science **309**, 268 (2005).
- ⁸ F. H. L. Koppens, J. A. Folk, J. M. Elzerman, R. Hanson, L. H. W. van Beveren, I. T. Vink, H. P. Tranitz, W. Wegscheider, L. P. Kouwenhoven, and L. M. K. Vandersypen, Science 309, 1346 (2005).
- ⁹ J. R. Petta, A. C. Johnson, J. M. Taylor, E. A. Laird, A. Yacoby, M. D. Lukin, C. M. Marcus, M. P. Hanson, and A. C. Gossard, Science 309, 2180 (2005).
- ¹⁰ J. Schliemann, A. Khaetskii, and D. Loss, J. Phys.: Condens. Matter **15**, 1809 (2003).
- ¹¹ G. Burkard, D. Loss, and D. P. DiVincenzo, Phys. Rev. B 59, 2070 (1999).
- ¹² S. I. Erlingsson, Y. V. Nazarov, and V. I. Fal'ko, Phys. Rev. B **64**, 195306 (2001).
- ¹³ S. I. Erlingsson and Y. V. Nazarov, Phys. Rev. B **66**, 155327 (2002).
- ¹⁴ A. Khaetskii, D. Loss, and L. Glazman, Phys. Rev. Lett. 88, 186802 (2002).
- ¹⁵ I. A. Merkulov, A. L. Efros, and M. Rosen, Phys. Rev. B 65, 205309 (2002).
- A. Khaetskii, D. Loss, and L. Glazman, Phys. Rev. B 67, 195329 (2003).
- $^{17}\,$ W. A. Coish and D. Loss, Phys. Rev. B $\,{\bf 70},\,195340$ (2004).
- ¹⁸ W. A. Coish and D. Loss, Phys. Rev. B 72, 125337 (2005).
- ¹⁹ A. S. Bracker, E. A. Stinaff, D. Gammon, M. E. Ware, J. G. Tischler, A. Shabaev, A. L. Efros, D. Park, D. Gershoni, V. L. Korenev, et al., Phys. Rev. Lett. **94**, 047402 (2005).
- ²⁰ M. V. Dutt, J. Cheng, B. Li, X. Xu, X. Li, P. R. Berman, D. G. Steel, A. S. Bracker, D. Gammon, S. E. Economou, et al., Phys. Rev. Lett. **94**, 227403 (2005).

- ²¹ D. Paget, G. Lampel, B. Sapoval, and V. I. Safarov, Phys. Rev. B **15**, 5780 (1977).
- ²² R. de Sousa and S. Das Sarma, Phys. Rev. B **67**, 033301 (2003).
- ²³ N. Shenvi, R. de Sousa, and K. B. Whaley, Phys. Rev. B 71, 224411 (2005).
- ²⁴ W. Yao, R.-B. Liu, and L. J. Sham, ArXiv Condensed Matter e-prints (2005), arXiv:cond-mat/0508441.
- ²⁵ A. M. Steane, Phys. Rev. A **68**, 042322 (2003).
- ²⁶ A. Imamoğlu, E. Knill, L. Tian, and P. Zoller, Phys. Rev. Lett. **91**, 017402 (2003).
- ²⁷ D. Paget, Phys. Rev. B **25**, 4444 (1982).
- Y. Kato, R. C. Myers, D. C. Driscoll, A. C. Gossard, J. Levy, and D. D. Awschalom, Science 299, 1201 (2003).
- ²⁹ G. Giedke, J. M. Taylor, D. D'Alessandro, M. D. Lukin, and A. Imamoøglu, ArXiv Quantum Physics e-prints (2005), arXiv:quant-ph/0508144.
- ³⁰ D. Stepanenko, G. Burkard, G. Giedke, and A. Imamoğlu, (unpublished).
- ³¹ J. Levy, Phys. Rev. Lett. **89**, 147902 (2002).
- ³² C. P. Slichter, *Principles of Magnetic Resonance* (Springer Verlag, Berlin, 1980).
- Although we only consider a pure state here, our treatment may be extended to an arbitrary mixed state by writing $\rho_I(0) = \sum_i p_i |\psi_i\rangle \langle \psi_i|$ with $|\psi_i\rangle = \sum_n a_n^i |n\rangle$. The diagonal elements of the nuclear spin system are then given by $\rho_I(n) = \sum_i p_i |a_n^i|^2$ and the continuum limit¹⁷ is performed as in the case of a pure state leading to the same results as for a pure state.
- ³⁴ B. H. Armstrong, J. Quant. Spectrosc. Radiat. Transfer 7, 61 (1967).
- ³⁵ A. M. Stoneham, J. Phys. D: Appl. Phys. **5**, 670 (1972).
- ³⁶ P. Minguzzi and A. di Lieto, J. Mol. Spectrosc. **109**, 388 (1985).
- ³⁷ H.-A. Engel, V. N. Golovach, D. Loss, L. M. Vandersypen, J. M. Elzerman, R. Hanson, and L. P. Kouwenhoven, Phys. Rev. Lett. **93**, 106804 (2004).
- $^{38}\,$ M. Borhani, V. N. Golovach, and D. Loss, condmat XXX.
- ³⁹ A. Barenco, C. H. Bennett, R. Cleve, D. P. Divincenzo, N. Margolus, P. Shor, T. Sleator, J. A. Smolin, and H. Weinfurter, Phys. Rev. A 52, 3457 (1995).